UXO Target Detection Using Magnetometry and EM Survey Data

Susan L. Rose-Pehrsson[a], Ronald E. Shaffer[a], J. R. McDonald[a], Herbert H. Nelson[a], Robert E. Grimm[b] and Thomas A. Sprott[b]

[a]Naval Research Laboratory, Chemistry Division, Code 6110, Washington, D.C. 20375-5342
[b]Blackhawk Geometrics, 301 Commercial Rd, Suite B, Golden, CO 80401

ABSTRACT

Digital filtering, principal component analysis (PCA), and an automated anomaly picker have been used to improve and automate target selection. This is the first step in a three part program to develop new data analysis methods to automate target selection and improve discrimination of unexploded ordnance (UXO) from clutter and ordnance explosive waste (OEW) using magnetometry (Mag) and electromagnetic induction (EM) survey data. Traditionally, target detection has been accomplished by a time-consuming manual interactive data analysis approach. Experts screen the magnetometer data and select potential UXO targets based on their intuitive experience. EM data has been used in a secondary role in this process and the anomaly picking included much classification and operator bias. In this program, the target detection step will use all of the data available and a separate classifier process will be used for identification and discrimination. Digital filtering is being used to enhance important features and reduce noise, while principal component analysis is being used to fuse three channels of data and reduce noise. Seven 50 meter-square data sets from the two test sites were used to investigate these techniques. Features of interest are enhanced using filtering techniques. Inspection of the first-principal component suggests that data fusion of the magnetometer and EM data can be successfully accomplished. The new image consisting of circular features of varying diameters and intensities represent significant features present in all three data channels. Data with strong magnetometer and EM signals have the greatest intensity and in most cases noise is reduced. An automated anomaly picker has been designed to select targets from Mag, EM and PCA images. The method is fast and efficient as well as providing user options to control pick criteria.

Keywords: Principal Component Analysis, target selection, UXO, digital filtering, data fusion, anomaly picker

1. INTRODUCTION

The Chemistry Division of the Naval Research Laboratory has developed the Multi-Sensor Towed Array Detection System (MTADS) to detect buried ordnance.[1] The system consists of a field-worthy, low magnetic signature vehicle and towed geophysical sensor arrays. Two sensor trailers are available; one has an array of eight cesium-vapor magnetometers and the other has an array of three time-domain electromagnetic induction sensors. The sensor data are positioned by a real-time, centimeter level accuracy GPS system and the data are recorded by a PC-based data acquisition system in the tow vehicle. After a site is surveyed, the data are transferred to a workstation-based Data Analysis System (DAS). The output of both trailers is three channels of data consisting of one magnetometer image and two EM images. Traditionally, targets are selected manually from a Mag or EM image of the site. The selected data is sent to a modeler based on a point dipole. The results of the model are evaluated for size and depth, and a dig sheet is generated for site remediation. This technology provides excellent detection with little discrimination. In addition, the targets sent to the modeler are highly operator dependent.

Locating, identifying and disposing of buried UXO on the 10 million acres of contaminated lands in the continental United States is a 500 billion dollar problem. Development of new technologies with improved data analysis has been identified as a high priority triservice requirement. Using current methods, it has been shown that false alarm detections far outnumber correctly identified ordnance. The best performing technologies typically have a false alarm rate of 300-500%.[2-5] The high cost of digging and disposing of targets accounts for the overwhelming portion of the costs of UXO remediation, therefore a substantial saving could be recognized if the number of false positives were reduced. Using data collected by the Naval Research Laboratory's MTADS, new software techniques are being developed to improve discrimination and reduce the false alarm rate. The program has three parts: Phase 1, Target Detection, Phase 2, Quantitative Modeling, and Phase 3, Target Classification. This paper describes Phase 1, Target Detection, in this three-part program.

Target Detection is focused on automation and inclusion of all available data. Manual target detection is time-consuming, requires an expect operator and is too difficult to consider more than one channel of data at a time. Experts screen the magnetometer data and select potential UXO targets based on their vast experience. Little use of the EM data is involved in this process and the manual anomaly picking includes much classification and operator bias. Ideally, the target detection step will use the all the data available, and since this program will have a separate classifier step, the automated target detection method need not include UXO classification. Subsequently, target identification, assignment of associated confidence levels, and classification will be done by the modeling and classification algorithms being developed in Phases 2 and 3 of this program. The goal of this program is to have the modeler-classifier operate on the maximum reasonable number of targets because computational power is not limited. Digital filtering and PCA methods are being developed to pre-process the data prior to automated anomaly picking. Digital filtering is being used to enhance important features and reduce noise, while principal component analysis is being used to fuse three channels of data and reduce noise. Automated methods have been developed to pick targets. For this program, the fundamental requirement for a successful automatic anomaly picker is that Type I error (missed detections) must be minimized, even if this means greater Type II error (selection of clutter for the modeler). The anomaly picker is designed such that minimal classification is imposed.

2. EXPERIMENTAL

The data used in this study were collected using NRL's MTADS from two sites: Badlands Bombing Range in South Dakota[6] and Blossom Point in Maryland[7]. At Blossom Point, NRL has created a site in which a variety of ordnance items have been buried. This site referred to as the Prove Out site and shown in figure 1 was used initially in all the studies due to its careful characterization. Three data channels, one Mag and Two EM, are being used. The data is processed using the MTADS DAS written in IDL 4 (Research System, Boulder, CO) and run on a Silicon Graphics Workstation. PCA methods were developed and studied using a Window95 version of IDL 5 on a PC. Gaussian filters and multiway PCA methods were investigated using MATLAB (The Math Works, Inc., Natick, MA). Magnetometer and EM surveys are projected on a x, y grid and the intensity of the signal are displayed in an image. An example of a site is shown in figure 1. Seven 50 meters square data sets or subsets of the sites were used for method development. The Fourier and wavelet filters and the automated anomaly picker were tested on the entire Badlands site using the MTADS DAS. Results of these studies were compared to manually generated dig sheets and the remediation results.

3. RESULTS AND DISCUSSION

The three-fold approach to target detection used here involves digital filtering, data fusion, and anomaly picking.

3.1 Digital Filters

Digital filtering methods have been applied to image processing to suppress unwanted noise and enhance the spatial features of interest. As applied to image processing, digital filtering is a neighborhood operation and in this work consists of a two dimensional window that is passed across the image pixel by pixel. The pixels in the windowed region are convoluted with the filter function specified by the user. The product is a new value for the pixel in the center of the window. This type of filtering is sometimes referred to as a sliding neighborhood operation.[8] These methods are particularly valuable to automated MTADS data processing when only one channel of data is available and PCA is not possible. The key to using this type of digital filtering is choosing the appropriate filter function and several different methods were investigated.

3.1.1 Gaussian

Gaussian and Laplacian of Gaussian (LoG) were investigated using the MATLAB filtering found in the Image Processing Toolbox[8]. For both types of filters, various widths and window sizes were studied to characterize the performance of the filters on MTADS images. MTADS data from the Prove Out and Badlands Sites were used to examine these methods. The routine *fspecial* allows the user to easily compute Gaussian and LoG filters of various widths and windows sizes. Once a filter function is defined, an image can be filtered using the *filter2* routine. These two routines were incorporated into a single MATLAB m-file *mifilt.m* (**M**ultivariate **I**mage **FILT**ering).

Gaussian and LoG filter were studied using sizes ranging from 5 to 50 and widths ranging from 3 to 20. Several trends were observed. Filtered images obtained using small widths and window sizes looked similar to the raw unfiltered images, while really large widths and window sizes completely suppressed the UXO signatures. In these initial investigations, widths of 10 and a window size of 25 appeared to be a good compromise. Figure 2 shows the scaled unfiltered image plots of mag, Em-1, and Em-2 from the Prove Out site and the filtered images. The Mag image data was obtained

using a LoG filter, while EM images were created using Gaussian filters. Comparing the filtered images with the unfiltered images, it is easy to see that filtering does enhance some of the smaller UXO signals. Keeping in mind that the linear filters used in these preliminary studies are quite primitive, better filters tuned to the UXO signatures should provide an even greater enhancement of the signal. The edge effects in the filtered images are an artifact of the linear filtering scheme used in this work and can be eliminated during the filtering process.

3.1.2 Fourier

Fourier filtering is well established in all forms of data and image processing.[9] A simple 2D band-pass technique, in which the amplitude filter is specified by minimum and maximum spatial frequencies and by a filter ramp coefficient are used here. The filter ramp controls the smoothness of the output image: when set to zero, the minimum and maximum frequencies are the boundaries of a boxcar-frequency filter and the resulting output image shows some spatial ringing. As the filter ramp is increased, cosine tapers are applied to the edges of the boxcar, and the filter shape approaches a Hanning window, which results in a smoother output image. The specified frequency range always applies to the center of the filter ramp. When combined with linear detrending applied to the whole image, Fourier filtering allows both small-scale noise and large-scale geological background to be rejected in favor of anomalies with spatial scales characteristic of UXO as shown in Figure 2.

3.1.3 Wavelets

Wavelets are more recent additions to signal processing.[10] Although both the Fourier and wavelet transforms return the same amount of information from a signal of length N, there are different trade-offs between spatial and spectral content. The Fourier transform densely samples the transform domain at spatial frequencies 1/L, 2/L, 3/L, ... where L is the physical length of the data. However, the sine and cosine basis functions of the Fourier transform are globally supported and do not spatially differentiate the signal. In contrast, the wavelet transform encodes spatial variations of scale length, but operates at fewer discrete frequencies 1/L, 2/L, 4/L.... For a 1024-sample signal, then there are 512 Fourier frequencies but only 9 wavelet scales. The choice of the actual length of the wavelet operator (often 4, 12, or 20 samples) determines the trade-off between spatial resolution and smoothness. Wavelets have found strong application in data compression: by choosing a discrete or ramped ("soft") cutoff in transform-coefficient magnitude, often 90% or more of the smallest coefficients can be eliminated and still retain the essential features of an image. In filtering, however, selection of features of interest, such as UXO-scale anomalies, and not the essential features of the image as a whole, which could contain significant non-UXO anomalies are desired. Hence it was found that coefficient thresholding using Daubechies wavelets was not very useful in the images tested. Therefore bandpass filters similar to those used in Fourier transforms were implemented. Whereas the dense frequency sampling by the Fourier transform allows the 2D frequency-domain filter to be approximately represented as an annulus, the more limited number of spatial scales in the wavelet forces this filter to look like a rotated "L". As shown in figure 3, the output signal from the wavelet bandpass looks squarish because wavelengths at arbitrary azimuths cannot be smoothly represented (the coordinate-axis directions are effectively oversampled), and because the Daubechies wavelets themselves are asymmetric in 2D. It appears that the utility of wavelet filters for UXO is limited, although further tests using smooth, zimuthally symmetric "halo" wavelets might yield better results.

3.2 Data Fusion

Multiway principal component analysis (mPCA) and PCA are the two methods investigated for data fusion of the three data channels. One goal of this research was to test PCA and the recently developed multiway principal component analysis (transform) algorithm, mPCA (or mPCT) for their ability to fuse the individual images from the MTADS system. It was hypothesized that the mPCA approach would provide better correlation between the images because the horizontal and vertical components of the images are treated separately.

3.2.1 Background

Conventional PCA analysis of multivariate images is well-understood methodology and is commonly used to process hyperspectral imagery data[11]. Each principal component, A, that is computed attempts to extract correlation (or variation) between the images. In terms of image analysis, the three MTADS images (Mag, EM-1, and EM-2) constitute a 3-dimensional matrix, $M \times N \times Q$, where M is the number of horizontal pixels (rows), N is the number of vertical pixels (columns), and Q is the number of images or sensors (in this MTADS example, Q = 3). It is assumed that the pixels at each x, y address in the three images refer to the same spatial location, otherwise fusion is not possible. The images are unfolded to a produce a two-dimensional matrix $(M \times N) \times Q$. Mathematically, the PCA algorithm can be written as

$$X = T \times P + E \quad (1)$$

where X is the unfolded image matrix, T is an (M×N)×A matrix of PC scores, P is an A × Q matrix of loadings or weights, and E is a matrix of residuals (variations or correlations not explained by the PCA model). Each column in T can be refolded back to image format to produce a PC scores image (M × N). The loadings for each PC are useful for interpretation.

While the PCA-image processing methodology is well understood, the unfolding and refolding processes cause a loss of spatial information. The rows in the X matrix could be randomly scrambled and the same loadings and scores would be computed. In attempt to regain the spatial information, mPCA was tested. One of the primary differences between PCA and mPCA is how the data is organized. In mPCA the images are reorganized to a Q × (M × N) matrix. Rather than decompose the data using singular value decomposition (SVD), the mPCA algorithm uses a trilinear decomposition. This approach utilizes separate SVD calculations for pixels in the horizontal and vertical directions. Mathematically, the mPCA image analysis can be written as

$$X = T \otimes P_x \otimes P_y + E \quad (2)$$

where X is the reorganized image matrix, T is a Q×A matrix of PC scores, P_x is a M × A matrix of loadings or weights, P_y is a N × A matrix of loadings or weights, and E is a matrix of residuals. To produce an image, the kronecker tensor product (⊗) of P_x and P_y is computed and unfolded.[12]

3.2.2 Multiway Principal Component Analysis Results

MTADS images from the Prove Out and Badlands sites were evaluated using the mPCA algorithm adapted for multivariate image analysis (*imagempca.m*) and coded in MATLAB. The protocol discussed above for reorganizing the data for the mPCA algorithm was used to pass the images to the *imagempca* routine. The resulting loading vectors (horizontal and vertical) were studied for the first PC. In both data sets, the first PC explained a majority of the variation in the images and no further components were computed. The loading vectors were then recombined to produced a fused image. Figure 4 shows a fused image from the Prove Out site. It is very clear from this image that the mPCA algorithm is not useful for image processing. Unlike the types of data in which the routine was designed, images cannot be written as linear combinations of the horizontal and vertical pixels. This assumption is valid for many applications of mPCA such as chemical sensor systems where the loadings refer to spectral (or sensor) and chromatographic profiles[13]. In image processing, the pixels in the horizontal and vertical directions have the same meaning, thus splitting them apart destroys the majority of the spatial information they contain. Based on these preliminary results no further experiments were conducted in this direction.

3.2.3 Principal Component Analysis Results

Using the pcomp function in IDL 5, PCA of magnetometer and EM data sets from the Prove Out Site were investigated. Examination of the image from the first principal component reveals features from each data set as shown in figure 5. This confirms the merger of the three channels of data into one image. Using the data sets from the Badlands site and Blossom Point sites, four variations in the analysis methods have been investigated. Sample covariance and sample correlation matrices were used with and without standardization. Standardizing the variables essentially makes them all 'equally important' by creating new variables with a mean of zero and variance of one. Standardization is important for these data sets since the magnitude of magnetometer and EM responses are significantly different. PCA using sample covariance and sample correlation matrices both with standardization are equivalent. Inspection of the first-principal component suggests that data fusion of the magnetometer and EM data is accomplished. The new image consists of circular features of varying diameters and intensities reveals features from all three data channels. Data with strong magnetometer and EM signals have the greatest intensity. In most cases, the targets present in the PCA image contained all the targets detected manually for both the Mag and EM data sets. In Badlands Image 1, a dry hole that was identified in the Mag image is not present in the PCA image as shown in figure 6. In the Blossom Point Site, several small nonordnance objects were not present in the PCA image that was detected in the EM image. These objects were small bits of wire and caps. The most important omission in the PCA image was observed in Badlands Image 3. In this case, a M38 bomb and Scrap present in the original Mag image was not present in the PCA image. Inspection of the EM images revealed that it was not present in those images either. Two EM images are used in the PCA application described here while only one Mag image is available. The EM results may be too heavily weighted for some types of data.

The goal was to fuse the data sets equally and not have one type of data be more significant than another at this phase of the analysis. Therefore studies were conducted to optimize the use of the PCA methods. Experiments were designed to

investigate how the variations in the data suites influence the results. Four approaches were used. In the first method, the above approach was used where all three data channels, Mag data plus both EM suites are combined in one PCA. The second method used only two channels of data, Mag plus EM1 for the PCA. In the third approach, first principal component was generated from four channels of data, Mag added twice plus both EM data suites. The fourth approach calculated the first principal component for only the two EM surveys, then combined that image with the Mag survey, and performed PCA again. All of the Badlands data sets as well as the Blossom Point data were evaluated in this study and the performance of the methods was compared with the dig sheets manually produced and the actual remediation results. The results of the study vary with differences in the data sets. In some cases, there is no difference between the approaches. Doubling the Mag signals was a poor choice due to numerical instabilities, which sometimes caused the system to crash. For the Blossom Point Site, all the PCA methods produced images that did not contain very small nonordnance targets, small bits of wire and caps. The PCA method that combined Mag with the first principal component of the two EM channels produced a similar image to Mag plus the first EM channel, expect the new image contained less noise as shown in figure 7. The same results were observed with the Badlands Image 4. The Badlands Image 3 provides the best evidence that the PCA method can be influenced by two EM channels as shown in figure 8. All the approaches that contained an equal number of Mag data channels as EM reveal two targets, a M38 and Scrap, that are present in Mag while not present in the EM surveys. In addition, the fourth approach combining PCA of Mag data with the first principal component of the EM surveys provides a clearer image with less background noise.

PCA was also applied to filtered data. Enhanced features are evident as shown in Figure 9. Figure 9a shows a PCA scores plot of the raw images, while Figure 9b shows a PCA scores plot of the filtered images. It is clear from these plots that a combination of filtering and PCA can be beneficial for this application.

3.3 Anomaly Pickers

The fundamental requirement for a successful automatic anomaly picker is that Type I error (missed detections) must be minimized, even if this means greater Type II error (selection of clutter for the modeler). The anomaly picker is designed such that minimal classification is imposed, although defining reasonable targets requires development of a selection criterion. The criteria will determine the target size for transport to the modeler. The anomaly picker also provides a user option where the exact parameters (threshold values) are determined interactively by the analyst.

Highlighting anomalies automatically in MTADS data is now possible with a tool called the autopicker, which uses parameters selected by the user and its own set of rules to draw outlines around anomalies. The full outline of an anomaly is more useful than a peak position or a circular approximation because it contains only the data that is needed by the modeler, reducing computation time and error. EM anomalies are traced differently than magnetic anomalies; EM will be treated first. In the first step, the autopicker uses a minimum threshold set by the user to select anomalies and anomaly groups. For an anomaly standing alone, the outer edge is determined by using a percentage of the peak value, providing the most efficient anomaly shape to the modeler. If anomalies are near enough to each other that the threshold operation groups them together, an uphill-walk algorithm isolates them. Every point in the group anomaly is the starting point for an uphill walk, following the steepest gradient until a peak is reached. The starting point is now associated with that peak and becomes part of a distinct anomaly. An example is shown in figure 10. Groups of peaks are nearly always separable by this method.

Picking magnetic anomalies requires additional steps due to the bimodal nature of the responses. The Mag responses have a positive and negative lope associated with each target. After the positive peaks are found as described for EM anomalies, the nearest point to the peak at amplitude zero or less is found and considered the zero-crossing point. Directions closer to the natural magnetic declination are favored. The picker proceeds past this point to the next local minimum on the same line, then finds the off-line minimum, which represents the negative peak. An inverted uphill-walk algorithm is used to delineate the negative lobe. It is not always possible to isolate negative magnetic lobes that overlap, but recently we have observed that the magnetic auto-picker works better if the negative lobes are selected first; i.e. the method described above is run in reverse. An example is shown in figure 11. Both of the EM and magnetic auto-pickers contain additional special-case rules; for example, it is desirable not to separate very close EM peaks because some EM anomalies are double-peaked due to the survey-coil geometry; the distance criterion is selectable by the user.

4. CONCLUSIONS

An investigation of linear filter functions was initiated to determine the feasibility and usefulness of these methods. Gaussian and Laplacian of Gaussian filter functions were applied to the Badlands and Blossom Point data sets. The filters

performed adequately and demonstrated new images with enhanced intensities and reduced noise. Gaussian filters performed best on EM surveys while Laplacian of Gaussian performed best on Mag data. Two types of filters have also been implemented in the MTADS DAS and investigated, Fourier and wavelet. The Fourier filters have demonstrated excellent results, while wavelets appear to have limited use in this application.

Preliminary studies indicate that mPCA cannot be used for fusion of multivariate images, while PCA methods demonstrated that they are useful in sensor fusion. Digital filtering followed by PCA also provided enhanced images using the Prove-out data set. The PCA method was tested on seven data sets from Blossom Point and the Badlands Sites. The images produced were compared to dig sheets to determine the accuracy of the results. In most data sets, all the targets that were determined in the early studies were also present in the new image. In a few cases, targets that later turned out to be dry holes, did not appear in the PCA image. In one of the images (Badlands Image 3), two targets, M38 and scrap, were not present in the PCA image. Since the targets were not present in the EM data sets, the PCA images appeared to be too heavily weighted to EM responses. When the study was repeated with only one EM suite of data, the PCA image had the targets present. The best approach to PCA seemed to be the combination of Mag with the PCA of both the EM surveys because in this case both types of data are weighted equally while taking advantage of all the data available. The images produced by this approach had sharper images and less background noise. Targets that were not present in the Badlands Image 3 when all three suites of data are used are present when the Mag data is added to the first principal component of the combined EM surveys.

A Beta Test version of the current MTADS DAS system is now complete and running at NRL. It has optional filtering, PCA analysis and the display of the first principal component image, and the ability to pick targets directly from the PCA, EM, or Mag images. The picker is fast and efficient. The entire Badlands Site can be processed in less than five minutes.

ACKNOWLEDGEMENTS

This work was supported by SERDP, project # CU-1092.

REFERENCES

1. **Need MTADS Reference**
2. "Unexploded Ordnance Advanced Technology Demonstration Program at Jefferson Proving Ground (Phase I)," U.S. Army Environmental Center, Report No. SFIM-AEC-ET-CR-94120, December 1994.
3. "Evaluation of Individual Demonstrator Performance at the Unexploded ordnance Advanced Technology Demonstration Program at Jefferson Proving Ground (Phase I)," U.S. Army Environmental Center, Report No. SFIM-AEC-ET-CR-95033, March 1995.
4. "Unexploded Ordnance Advanced Technology Demonstration Program at Jefferson Proving Ground (Phase II)," U.S. Army Environmental Center, Report No. SFIM-AEC-ET-CR-96170, **??**.
5. J.R. McDonald, H.H. Nelson, and R. Robertson, "Results of the MTADS Technology Demonstration at the Magnetic Test Range", Marine Corps Air Ground Combat Center (MCAGCC), Twenty-nine Palms, CA, NRL/PU/6110-97-**XXX, in press**.
6. J.R. McDonald, H.H. Nelson, J. Neese, R. Robertson and R.A. Jeffries, "MTADS Unexploded Ordnance Operations at the Badlands Bombing Range," Pine Ridge Reservation, Cuny Table, S.D., NRL/PU/6110-98-353, July 1997.
7. **Blossom Point Ref**
8. "MATLAB Image Processing Toolbox User's Guide", Mathworks, Inc., Natick, MA, 1997.
9. IDL Reference Guide
10. **REF Numerical Recipes??**
11. K. Esbensen and P. Geladi, Strategy of Multivariate Image Analysis, *Chemometrics and Intelligent Laboratory Systems*, 7, 1989, 67-86.
12. "Multiway Calibration. Multilinear PLS," R. Bro, **J. Chemometrics, 10,** 47 (1996)
13. R.E. Shaffer, S.L. Rose-Pehrsson, R.A. McGill, Multiway Analysis of Preconcentrator-Sampled Surface Acoustic Wave Chemical Sensor Array Data, *Field Analytical Chemistry and Technology*, accepted.

FIGURES

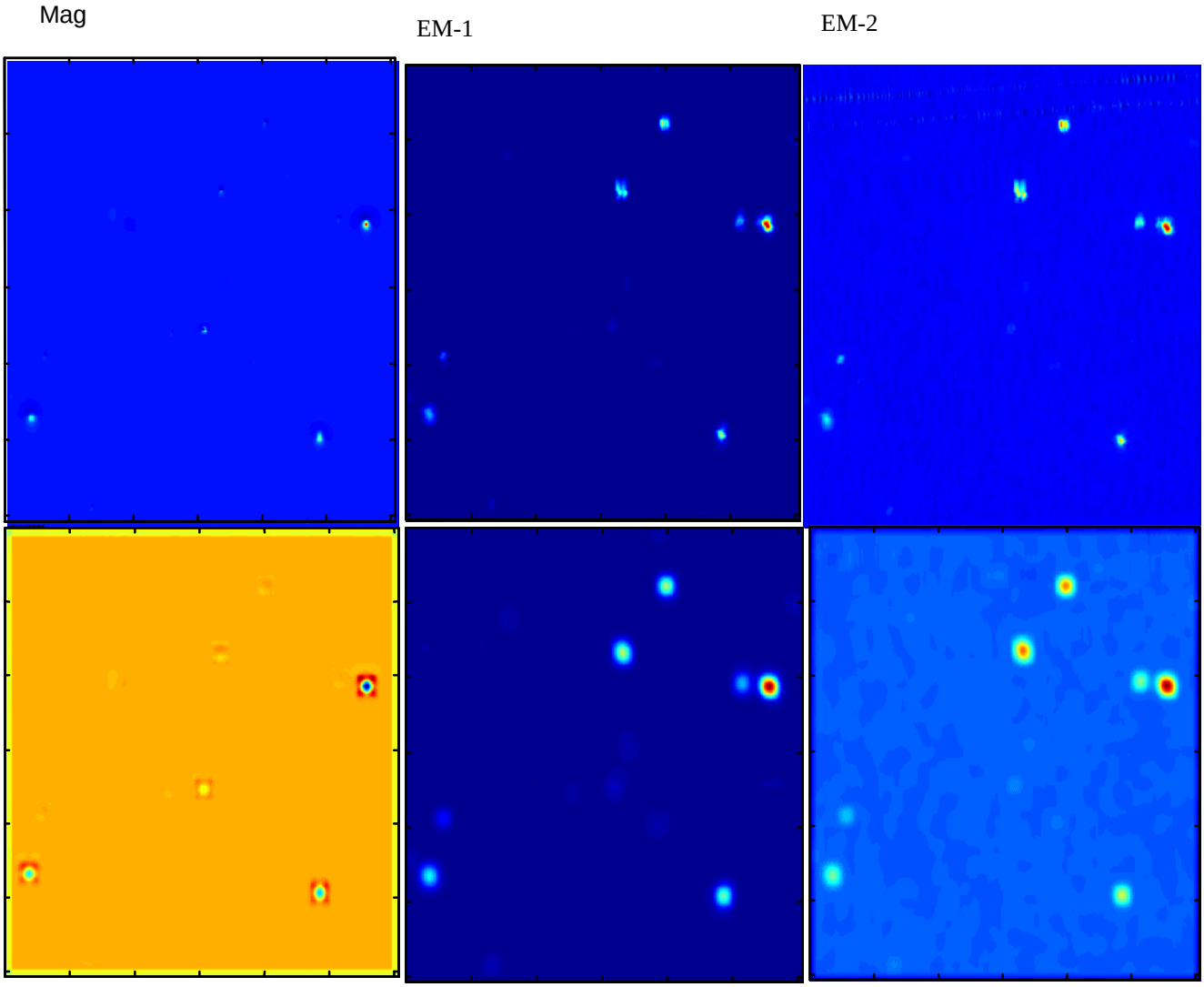

Figure 2. Raw and Filtered images from Badlands Bombing Range. The filtered images on the bottom provide enhanced features and reduced background noise. LoG filter used for Mag data, while Gaussian used for EM surveys.

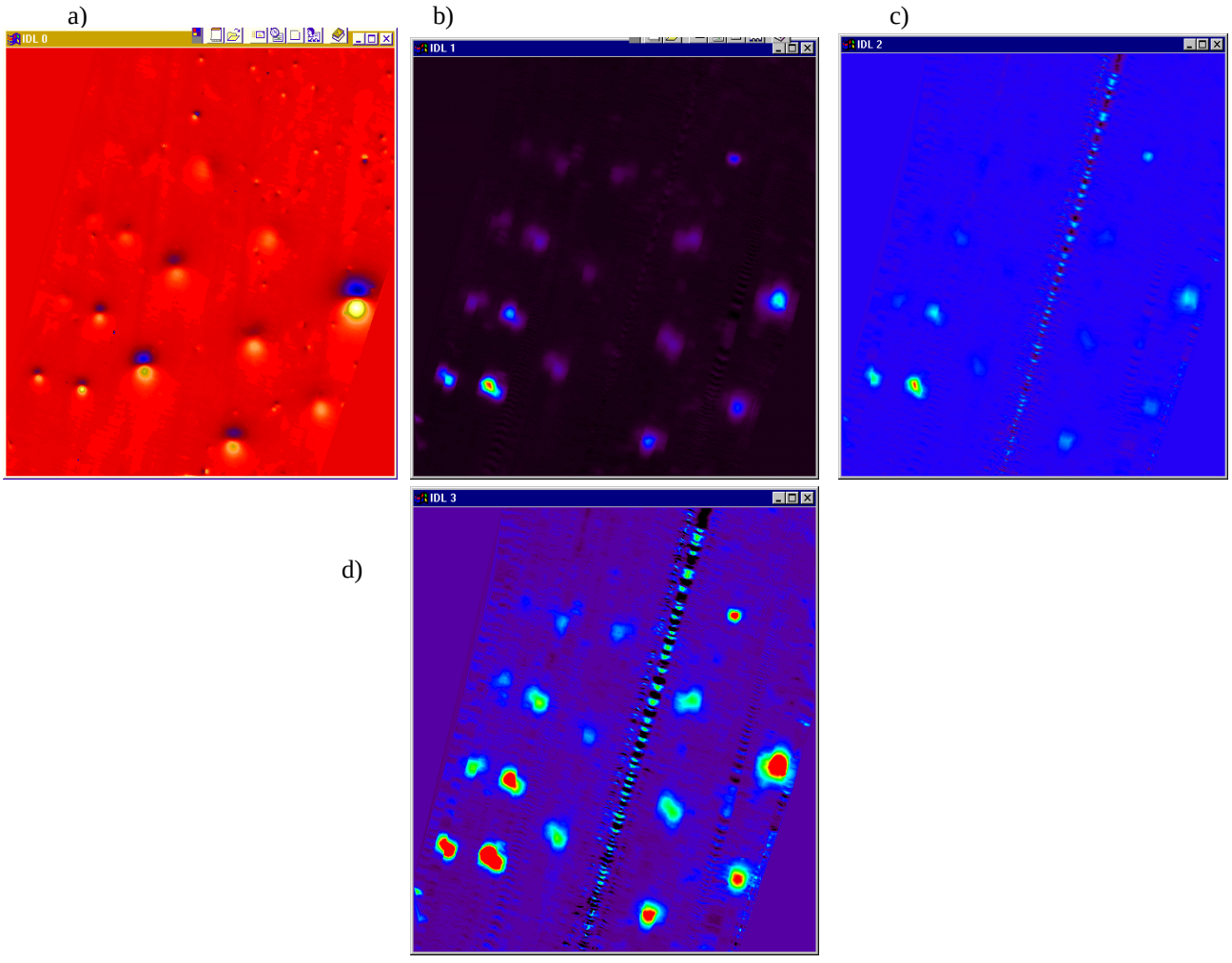

Figure 1. Mag (a) , EM1 (b), EM2 (c) and PCA (d) images from the Prove Out Site at Blossom Point. The PCA image (d) reveals important features from each data channel.

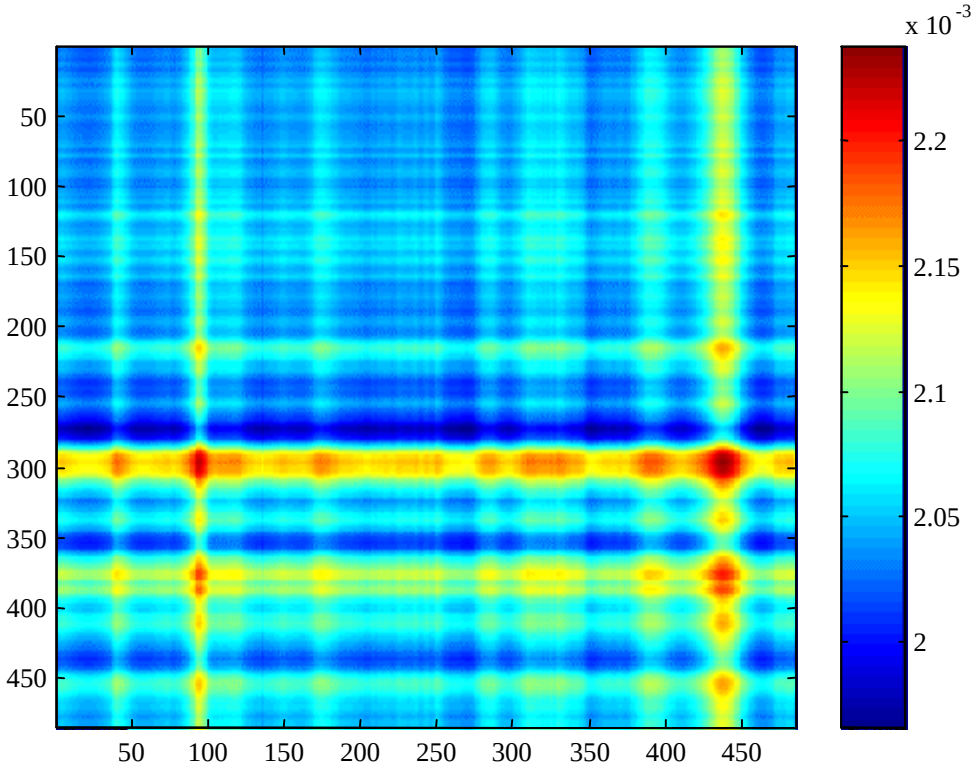

Figure 5. Results of the mPCA study displaying the image of Prove Out Site data set.

a) b)

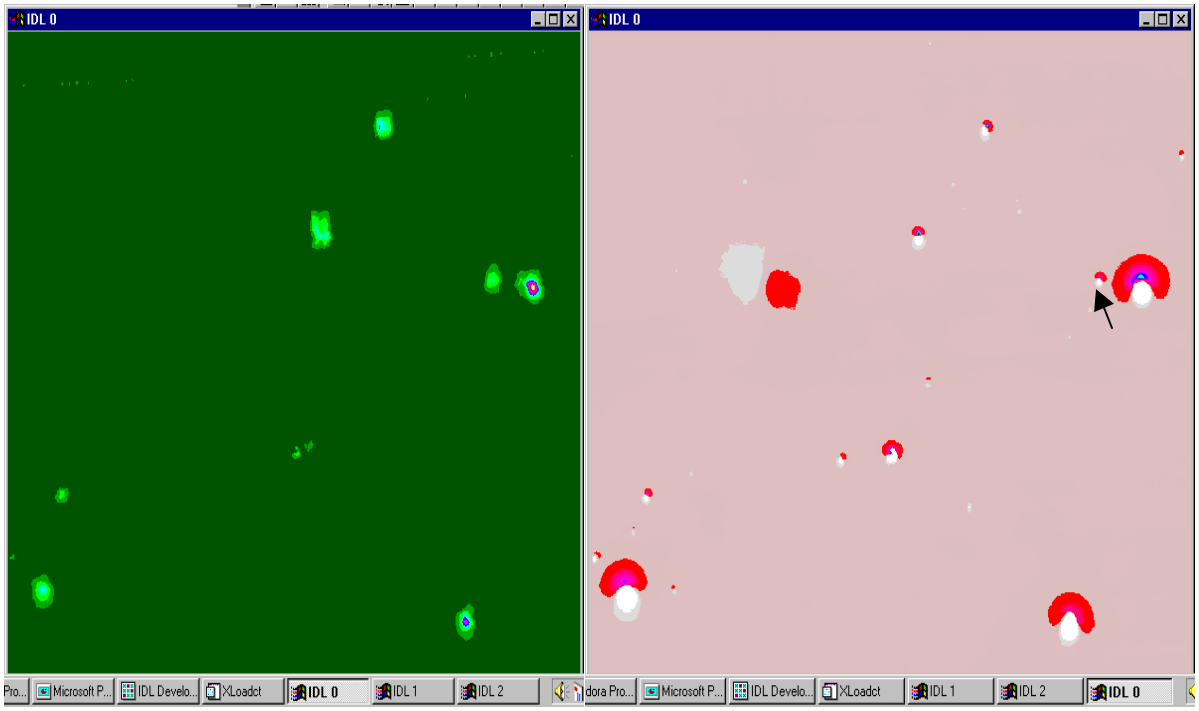

Figure 6. Badlands Image 1. Dry Hole (target 436) shown in the Mag image (b) is not present in PCA image (a).

a) b) c)

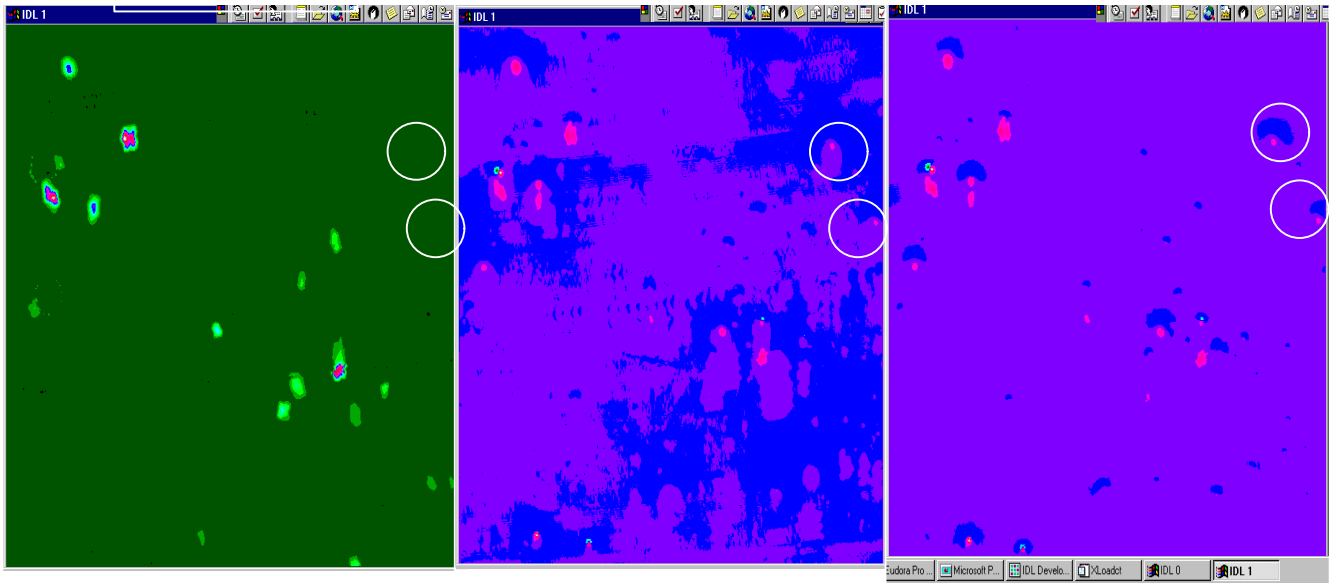

Figure 7. Badlands Image 3. a) PCA of all three channels has two targets missing. b) PCA of Mag and EM1 has targets present. c) The targets are present plus the noise is reduced when PCA is done in two steps, first on the two EM surveys, then on the first principal component of both EM surveys and the Mag data.

a) Raw b) Filtered

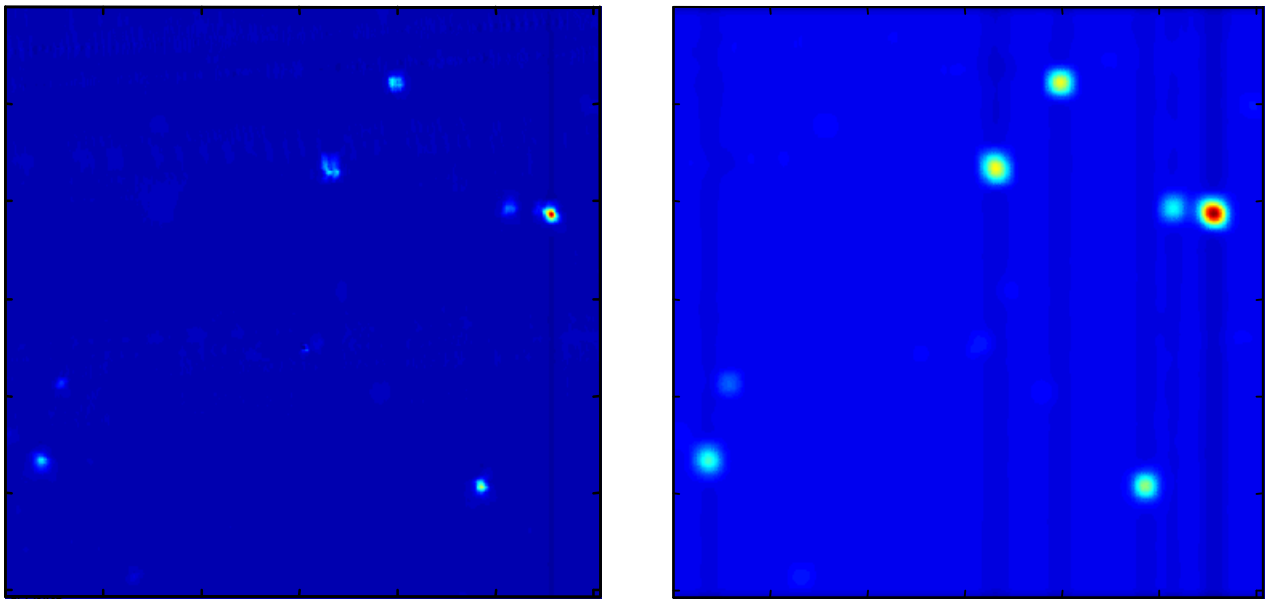

Figure 8. An example of PCA images for both raw (a) and filtered (b) data. In this Badlands image enhanced features are clearly observed for the filtered data.

a) b)

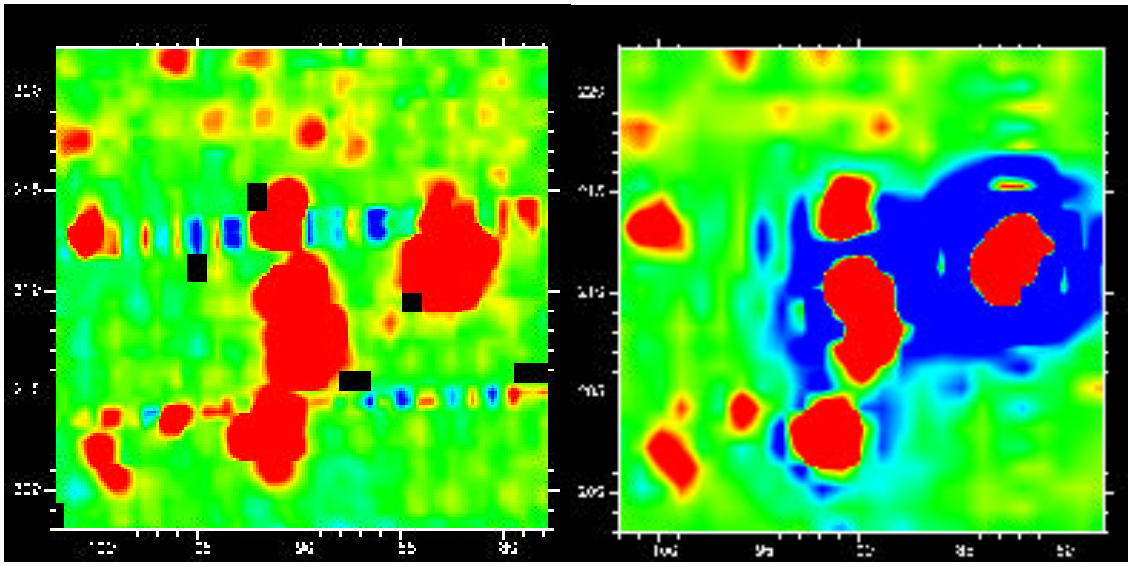

Figure 3. (a)"Raw" image of EM data, 20-m square, from Badlands Bombing Range (BBR), full-scale range -20 to +50 mV. Large anomalies are displayed in saturation to accentuate small-scale noise and vehicle chatter. (b) Fourier-filtered version of image (lowpass wavelengths of 2 m and longer—i.e., frequency less than 0.5 1/m—filter ramp 0.4 1/m).

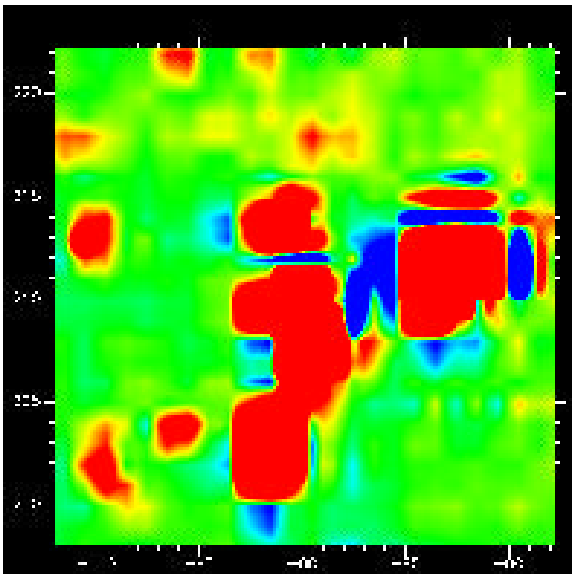

Figure 4. Wavelet-filtered version of Fig. 3 (Daubechies-4 wavelet, lowpass length scales 4 m and longer). Standard wavelets, while well suited to finding the most important features of a scene (image compression), give discretized and squarish outlines as filters.

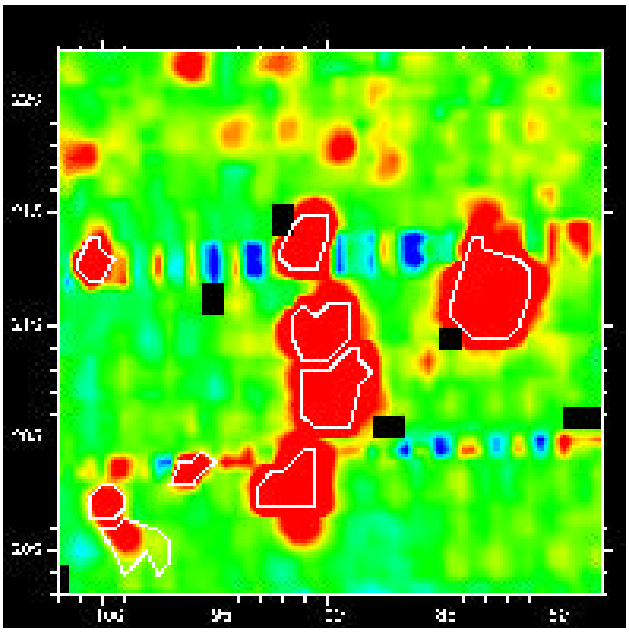

Figure 9. Autopicker results on Fig. 3 (threshold 5 mV, base fraction 0.1, minimum anomaly separation 1.2 m; see text for explanation). The autopicker is designed to trace individual anomaly shapes as best as possible, including closely spaced anomalies, in order to select spatially associated ungridded data for subsequent presentation to modeling and discrimination algorithms (note angular shape of bottom anomaly is due to a gridding artifact).

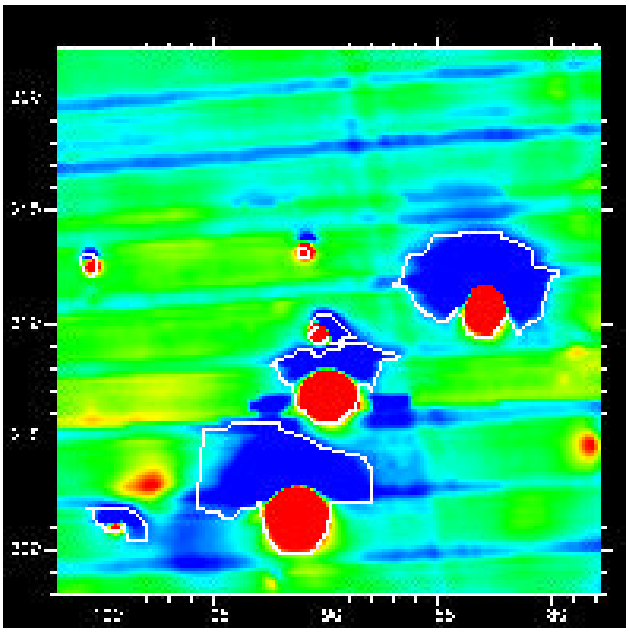

Figure 10. Autopicker results on magnetic image of same area as previous figure (threshold 20 nT, minimum signal 7 nT, minimum anomaly separation 1.2 m; see text for explanation). Magnetic autopicker must form dipoles by associating low with high anomalies.